Somatic PIK3R1 Variation as a Cause of Vascular Malformations and Overgrowth

Journal: Genetics in Medicine

Title: Somatic *PIK3R1* Variation as a Cause of Vascular Malformations and Overgrowth

Authors: Catherine E. Cottrell PhD[1]; Nicole R. Bender MD[2]; Michael Zimmerman MD[3]; Jonathan Heusel MD, PhD[4]; Meagan Corliss MS[4]; Michael Evenson MS[4]; Vincent Magrini PhD[1]; Donald J. Corsmeier DVM[1]; Matthew Avenarius[5]; Jeffrey N. Dudley[6]; Jennifer J. Johnston PhD[7], Marjorie J. Lindhurst PhD[7], Katinka Vigh-Conrad PhD[8]; Olivia M.T. Davies BS[3]; Carrie C. Coughlin MD[4]; Ilona J. Frieden MD[9]; Megha Tollefson MD[10]; Andrea L. Zaenglein MD[11]; Heather Ciliberto MD[12]; Laura L. Tosi MD[13]; Robert K. Semple MB PhD[14]; Leslie G. Biesecker MD[7]; Beth A. Drolet MD[15]

[1]The Steve and Cindy Rasmussen Institute for Genomic Medicine at Nationwide Children's Hospital, Columbus, OH, [2]University of Florida, Gainesville, FL, [3]Medical College of Wisconsin, Milwaukee, WI, [4]Washington University School of Medicine, Saint Louis, MO, [5]Department of Pathology and Laboratory Medicine, The Ohio State University Wexner Medical Center, Columbus, OH, [6]University of Michigan Medical School, Ann Arbor, MI [7]Medical Genomics and Metabolic Genetics Branch, National Human Genome Research Institute, Bethesda, MD, [8]Oregon Health & Science University, Portland, OR, [9]University of California-San Francisco, San Francisco, CA, [10]Mayo Clinic, Rochester, MN, [11]Dermatology and Pediatrics, Penn State Hershey Medical Center, Hershey, PA, [12]Town Square Dermatology, Coralville, IA, [13]Division of Orthopaedics & Sports Medicine, Children's National Hospital, Washington, DC [14]University of Edinburgh, Edinburgh, United Kingdom, [15]University of Wisconsin-Madison School of Medicine and Public Health, Madison, WI

Corresponding Author: Dr. Beth A. Drolet
Address: One South Park Street, 7th Floor
Madison, WI 53715
Tel: 608-287-2620
Fax: 608-287-2676
Email: bdrolet@dermatology.wisc.edu

Funding Sources:
LGB was supported by the Intramural Research Program of the National Human Genome Research Institute, grants HG200328 and HG200388. RKS was supported by the Wellcome Trust, grant 210752/Z/18/Z.

Key words: PIK3R1, Overgrowth, CLOVES Syndrome, Klippel-Trenaunay Syndrome, Vascular malformation, PI3K, AKT, Cancer, Next-generation sequencing, Limb malformations, Capillary malformation

Conflict of Interest Notification Page

Conflicts of Interest:
Beth A. Drolet: Venthera, Clinical Advisory Board, Consultant, Co-founder Pediatric Derm development, LLC.

Ilona J. Frieden: Venthera, Clinical Advisory Board, Novartis, Consultant, Pfizer Inc., Data Safety Monitoring Boards

Leslie G. Biesecker: Illumina Corp, Ethics Advisory Board

Jonathan W. Heusel: PierianDx, Knowledgebase Expert Panel member

All other authors declare no conflicts of interest.

Financial Disclosures:
Leslie G. Biesecker: has received in-kind research support from ArQule, Inc. (now wholly owned by Merck, Inc.), Novartis, and Pfizer Inc., royalties from Genentech, Inc, and honoraria from Cold Spring Harbor Press.

Beth A. Drolet: has received in-kind research support from Venthera and research support for an investigator-initiated retrospective on oral propranolol from Pierre Fabre.

Robert Semple has received in-kind research support from Pfizer, Inc.

Laura L. Tosi has received research support from Ultragenyx Pharmaceutical.

ABSTRACT

Purpose: Somatic activating variants in the PI3K-AKT pathway cause vascular malformations with and without overgrowth. We previously reported an individual with capillary and lymphatic malformation harboring a pathogenic somatic variant in *PIK3R1*, which encodes three PI3K complex regulatory subunits. Here, we investigate *PIK3R1* in a large cohort with vascular anomalies and identify an additional 16 individuals with somatic mosaic variants in *PIK3R1*.

Methods: Affected tissue from individuals with vascular lesions and overgrowth recruited from a multi-site collaborative network was studied. Next-generation sequencing targeting coding regions of cell-signaling and cancer-associated genes was performed followed by assessment of variant pathogenicity.

Results: The phenotypic and variant spectrum associated with somatic variation in *PIK3R1* is reported herein. Variants occurred in the inter-SH2 or N-terminal SH2 domains of all three PIK3R1 protein products. Phenotypic features overlapped those of the PIK3CA-related overgrowth spectrum (PROS). These overlapping features included mixed vascular malformations, sandal-toe gap deformity with macrodactyly, lymphatic malformations, venous ectasias, and overgrowth of soft tissue or bone.

Conclusion: Somatic *PIK3R1* variants sharing attributes with cancer-associated variants cause complex vascular malformations and overgrowth. The *PIK3R1*-associated phenotypic spectrum overlaps with PROS. These data extend understanding of the diverse phenotypic spectrum attributable to genetic variation in the PI3K-AKT pathway.

INTRODUCTION

Vascular malformations and the overgrowth syndromes of which they are commonly a part constitute a heterogeneous group of congenital malformations that lead to significant morbidity and disfigurement. Next-generation sequencing (NGS) has become an important tool in genomic investigation of these syndromes, allowing improved molecular characterization and diagnosis. Developments in NGS technology have enabled successful discovery of disease-associated somatic variation within affected tissue.[1,2] It is now recognized that vascular malformations and overgrowth demonstrate some shared genetic variation with cancer, with the phosphoinositide 3-kinase (PI3K)-AKT growth signaling pathway commonly dysregulated in both sets of disease.[3-5]

Class I phosphatidylinositol 3-kinases (PI3K) function as heterodimers composed of a catalytic and a regulatory subunit and serve as intracellular signal transducers that convert phosphoinositide (4,5)-bisphosphate into phosphoinositide (3,4,5)-trisphosphate (PIP3). PIP3 generation triggers activation of downstream effectors including PDK1 and then AKT, which promote cell growth and survival.[6] Somatic mosaic activating variants in *PIK3CA*, encoding the p110α catalytic subunit of the PI3K heterodimer, have been well-described in vascular malformations and overgrowth syndromes.[7] Among the regulatory subunits of PI3K, *PIK3R1* encodes three distinct protein products (p85α, p55α and p50α), generated through alternative splicing. These products form obligate heterodimers with PIK3CA, stabilizing and inhibiting it in the basal state, while mediating its binding to activated receptor tyrosine kinases and its subsequent activation.[8] PIK3R1 also negatively regulates the PI3K pathway by stabilizing the phosphatase PTEN, itself a tumor suppressor.[9]

PIK3R1 variants that fail to inhibit p110α activity, usually by disruption of the inter-SH2 domain, cause constitutive PI3K pathway activation, and are enriched in cancers, albeit much less commonly than *PIK3CA* variants. Given the numerous variants identified in PI3K pathway components (*PIK3CA*, *AKT1*, and *PTEN)* in overgrowth, *PIK3R1* is an excellent

candidate gene for vascular malformations and overgrowth. We used targeted, high-depth NGS to analyze affected tissue from a cohort of individuals with vascular malformations, and thereby extend understanding of the role played by *PIK3R1* in these clinically important disorders.

MATERIALS AND METHODS

Study cohort

The study was authorized by the institutional review board of participating institutions. Individuals described herein were identified to harbor a variant in *PIK3R1* amid the setting of apparently mosaic disease and were derived from one of three cohorts which together enabled the assemblage of variant and phenotype data within this described study cohort. The primary cohort is a multi-site network coordinated through the Pediatric Dermatology Research Alliance (PeDRA)[3] enrolling patients of any age with vascular anomalies and overgrowth. Specimens were available on 108 patients consisting of 3-4 mm skin punch biopsy samples from affected tissue or a paraffin-embedded sample of affected tissue from previous excisions. Within the PeDRA cohort, ten *PIK3R1*-variant positive individuals were identified. Among a National Institutes for Health (NIH) cohort of 297 individuals ascertained for heterogeneous manifestations of vascular anomalies and overgrowth, two *PIK3R1*-variant positive individuals were identified. The NIH cohort eligibility criteria were apparently mosaic (segmental) overgrowth of extra-central nervous system (CNS) organs/tissue. Individuals may or may not have had CNS manifestations, but those with CNS manifestations alone were not included, nor were those with vascular anomalies alone without other manifestations of overgrowth. Samples collected for sequencing included either punch skin biopsies of apparently affected tissues or excisional biopsies collected at the time of surgery. Of necessity, these samples were highly heterogeneous in nature and number, based on the clinical needs and limitations of the individuals. The Genomics and Pathology Services (GPS) at Washington University School of Medicine cohort consisted of five *PIK3R1*-variant positive individuals ascertained from a total of 343 individuals assayed clinically for suspected disorders of somatic mosaicism, including but not limited to, overgrowth and vascular

malformation. Where available, clinical data were retrospectively collected and included medical history, dermatologic and musculoskeletal exams, and clinical and radiologic images. Available clinical and radiologic images were reviewed centrally. The NIH study was reviewed and approved by the NHGRI IRB, protocol number 94-HG-0132.

Sequencing Methodologies

Next-generation sequencing (NGS) was utilized in all centers to identify genetic variation (supplemental methods). DNA was extracted from affected fresh frozen tissue (FT), cultured tissue (CT) or from formalin-fixed paraffin-embedded (FFPE) blocks of previously excised affected tissue.

RESULTS

Identification of pathogenic variants in *PIK3R1*

PIK3R1 variants were detected in tissue of 17 individuals within the study cohort, and were observed at a reduced variant allele frequency/fraction (VAF) consistent with a somatic etiology, with most detected at less than 10% (Table I). The identified variants included missense and insertion-deletion (indel) variants within the SH2 (n=1) and PI3K_P85_iSH2 (n=16) domains of PIK3R1 and overlapped regions harboring known hotspots seen in cancers (Figure 1).[10-12] Notably, the variants detected in vascular malformation and overgrowth occur in domains that are common to all PIK3R1 products (p85α, p55α and p50α). Recurrent variation was detected among this cohort resulting in nine unique variants at the level of the coding sequence, and seven unique variants at the level of the predicted protein consequence. Indel events comprised three in-frame deletions and four splice-site alterations.

Variant Attributes

Variants were interpreted using a modification of the American College of Medical Genetics and Genomics and the Association for Molecular Pathology (ACMG/AMP) standards and guidelines for variant interpretation as described in the supplemental methods.[13] Variants were considered to be of somatic origin if the variant allele was observed at a diminished VAF or a

variant was present at differing frequencies among tissues from the same individual. Variant attributes considered when assessing for pathogenicity included variant location within the gene or protein product (hotspot or domain), occurrence and frequency within this cohort, and within the wider setting of human disease, as well as variant type and predicted impact on the protein product. Among the detected variants, 15 were classified as pathogenic (five of these being unique at the level of the predicted amino acid change), with two classified as likely pathogenic.

Clinical phenotype in individuals with *PIK3R1* pathogenic variants

Expert-reviewed clinical images and data were available for 12 individuals harboring *PIK3R1* variants, and their phenotypes were similar to those attributed to somatic mosaic hotspot variants in *PIK3CA*. Most patients had red vascular stains (10/12), venous ectasias or engorgement (11/12), and mild soft tissue or bone overgrowth (11/12). Four individuals had sandal-toe gap deformities of the foot with mild macrodactyly of the second toe. (Table II, Figure 2). Other clinical features noted included developmental delay, cutaneous syndactyly, and lipoma/fatty tissue overgrowth. Among individuals in whom extensive phenotype information was available (PeDRA cohort, n=10; NIH cohort, n=2), seizures, macrocephaly or hydrocephalus were not described. Individuals had been previously diagnosed with various acronyms or eponyms including: Klippel-Trenaunay Syndrome, CLOVES syndrome, and PROS.

DISCUSSION

PIK3R1 is ubiquitously expressed and has important roles in physiology and disease. It encodes the p85α, p55α and p50α regulatory subunits of class 1A PI3K, which bind tightly to any of the p110α, β or δ catalytic subunits. It is the p110α subunit, encoded by *PIK3CA*, which is by far the most commonly mutated and activated in cancer and overgrowth syndromes. PI3K transduces cell surface activation of receptor tyrosine kinase growth factor and hormone receptors into downstream activation of AKT and other pathways to regulate cell metabolism,

size, differentiation, proliferation, migration, and apoptosis.[14,15] The PI3K/AKT pathway is constitutively activated in affected tissue from many vascular malformations,[1,16,17] primarily through mosaic variation in *PIK3CA,* as in cancer.

PIK3R1 variation in the setting of vascular malformation with overgrowth has been rarely reported. We previously described a single individual harboring a somatic mosaic *PIK3R1* variant, p.(Lys567Glu), with capillary and lymphatic malformation, and leg length discrepancy (individual 4 as referenced in this cohort).[3] A further patient harboring a *PIK3R1* iSH2 domain variant, p.(Asn564Lys), was reported to have macrocephaly, tracheomalacia and cardiovascular malformation described by the authors as in the context of megalencephaly-capillary malformation (MCAP) syndrome, as well as recurrent infections in keeping with Activated PI3K-Delta Syndrome 2 (APDS2).[18] We confirm in a large cohort that somatic mosaic *PIK3R1* variants are a significant cause of vascular malformation and overgrowth. The phenotypes observed in individuals with somatic mosaic variants in *PIK3R1* are similar to those associated with mosaic *PIK3CA* hotspot variants. All individuals with mosaic *PIK3R1* variants had red-purple, geographic vascular stains, most with associated venous engorgement, venous prominence and soft tissue or bone overgrowth, but this tended to be mild and relatively uniform. One individual with a unique variant within the N-terminal SH2 domain, p.(Gly376Arg), had a light pink reticulate vascular stain with associated limb undergrowth. Residue 376 has been designated as a cancer hotspot, with the variant itself, p.(Gly376Arg), functionally characterized as capable of inducing in-vitro oncogenic transformation and activation of p110α. [19,20]In total, the observed clinical features among the individuals assembled within our cohort suggests that somatic mosaic variants in *PIK3R1* activate the PI3K pathway, however the degree of activation, particularly in comparison to disease-associated variation in *PIK3CA*, requires further study.

As is the case for somatic mosaic overgrowth-associated variants in *PIK3CA* and *AKT1*, mosaic *PIK3R1* variants are also found in cancer.[21] *PIK3CA* is more commonly altered in cancer in comparison to *PIK3R1.* Among 181 studies with non-redundant samples curated in cBioPortal

encompassing in total 47,580 samples, 10.3% harbored a *PIK3CA* variant, as opposed to 2.1% for *PIK3R1* (date accessed 11-11-2020). Among this curated dataset, in-frame variants were more common in *PIK3R1,* (22.2% of all variants), than in *PIK3CA*, (2.5% of all variants). Similarly, in our PeDRA multi-site network with vascular anomalies and overgrowth, *PIK3R1* variants were less common (9.2%, 10/108) than variants in *PIK3CA* (39.8%, 43/108 individuals), with notable enrichment of in-frame variants in *PIK3R1* (Supplemental Figure 1).

Constitutional variants in *PIK3R1* have been shown to exhibit striking genotype-phenotype correlation. Most pertinent to this study, variants disrupting canonical splicing of exon 11 and leading to in-frame deletions in the N-terminal of the inter SH2 domain cause APDS2, an immunodeficiency characterized by recurrent infections and lymphoproliferation.[22] Hyperactivation of PI3K signaling in APDS2 has been demonstrated in lymphocytes, yet despite ubiquitous expression of the pathogenic variant, associated overgrowth has been exceedingly rarely described.[18,23] In vitro studies have shown that APDS2 variants in *PIK3R1* cause distinct patterns of hyperactivation of p110δ, the dominant lymphocyte catalytic subunit, and p110α, the ubiquitous growth-promoting subunit, based on subtle differences in the inhibitory molecular interactions of the regulatory and catalytic subunits: although both are hyperactivated, basal hyperactivation of p110δ was greater than 300 fold, while basal activation of p110α was only 2 fold.[24] This establishes that subtle differences in molecular interactions at the dynamic interface of regulatory and catalytic subunits can have major effects on the pattern of biochemical activation of mutant holoenzyme. This has yet to be studied for vascular and overgrowth-related *PIK3R1* variants, but it is plausible that these, too, result in a distinct profile of biochemical activation of different catalytic subunits. A full account of biochemical differences will also have to address any effects of variations in PI3K subunit expression and stoichiometry in various tissues, which is known to modulate PI3K activity.

In the aforementioned individual described with features of APDS2 and MCAP, the pathogenic heterozygous *PIK3R1* variant, p.(Asn564Lys), was associated with mildly increased

lymphocyte AKT phosphorylation.[18] A different missense change at codon 564, p.(Asn564Asp), was the most frequently detected variant in our vascular malformation and overgrowth cohort and is also described in cancer. Interestingly, in biochemical studies it has been shown to increase basal activity of p110α and β significantly more than δ, a pattern opposite to that described for the APDS2 variant, albeit in a different experimental paradigm.[25] Overt clinical manifestations of immune dysregulation were not identified in any of the individuals within our cohort, however; most patients did not undergo systematic laboratory evaluation for abnormalities in B cells and T cells.

In contrast to APDS2, constitutional *PIK3R1* loss-of-function variants, predominantly in the C-terminal SH2 domain, have been shown to cause SHORT syndrome (Short stature-Hyperextensibility-hernia-Ocular depression-Rieger anomaly-Teething delay).[26] These variants disrupt association of PI3K holoenzyme with activated RTKs, leading to downstream hypostimulation of the PI3K/AKT axis in response to ligand stimulation. The phenotype is correspondingly the "inverse" of vascular malformations and overgrowth, including intrauterine growth restriction, lipoatrophy, and insulin resistance/diabetes.[27] Of note, very rare reports of phenotypic overlap have been described between APDS2 and SHORT syndrome.[28] In principal, these findings suggest that there are largely distinct spectra of *PIK3R1* variants associated with these three disorders. Biochemical studies demonstrate that differences between SHORT syndrome and APDS2 are attributable to different profiles of activation or repression of PIK3CA and PIK3CD by mutant *PIK3R1* products.

The mutational spectrum of *PIK3R1*-related somatic mosaic overgrowth is largely distinct from the constitutional *PIK3R1*-related disorders, and no apparent loss of function variants were seen among 17 unrelated affected individuals. Recurrent missense variants were identified, with one variant observed in affected tissue from three individuals, p.(Lys567Glu), and one variant in six individuals, p.(Asn564Asp). Indel variants were a frequent observation within this cohort with 7/17 (41%) variants of this type detected. These included three predicted in-frame events and

four splice-site alterations, the latter recurrently located at the intron 13/exon 14 junction (NM_181523.3) (Supplemental Figure 2, Supplemental Table I). Due to the genomic architecture in this region, codon 582, which encodes a methionine, is split across exons 13 and 14. Furthermore, the intron 13/exon 14 junction consists of a spanning GGT sequence which is repeated once in exon 14. Genomic complexity and variability in published variant descriptions within this region further confound interpretation. Based solely on the observed sequencing data and established bioinformatic and nomenclature conventions, we would describe one such variant, c.1748_1750del, as predicted to encode p.(Trp583del). Notably, this variant has been reported previously in cancer literature and databases described as Trp583del, or as a splice variant affecting methionine codon 582.[10,29,30] In cancer studies, RNA sequencing demonstrates that variably sized indel splice variants impacting the splice acceptor (described as M582_splice) result in in-frame exon 14 skipping.[11] Based on these data, the protein consequence of these exon 14 skipping variants should be described as p.(Met582_Asp605delinsIle).

Both simple and complex indels are enriched in *PIK3R1* at recurrent genomic regions defined as hotspots occurring within discrete clusters within the SH2 and inter SH2 domains, with demonstrated statistical significance observed from large cancer datasets (Supplemental Table I) (cancerhotspots.org).[11,12,31] One such variant in our cohort, p.(Gln579_Tyr580del), has been shown to demonstrate nearly two-fold increased activity as measured by an *in vitro* phosphatidylinositol phosphorylation assay, retaining p110α binding but losing inhibitory activity.[25,32] Further studies to establish the activation pattern conferred by *PIK3R1* variants associated with vascular malformations and overgrowth are needed. Moreover, characterization of *PIK3R1* variants and functional impact are of particular importance in consideration of treatment. The application of targeted therapeutics has been previously investigated in the setting of vascular malformation and somatic overgrowth. Importantly, studies of alpelisib, a targeted inhibitor of p110α, have demonstrated efficacy in PROS with attenuation of disease

symptomology and may reasonably be considered for further study in the setting of *PIK3R1* variation.[33]

The somatic mosaic *PIK3R1* variants we describe in vascular malformations and overgrowth further extend our understanding of *PIK3R1,* whose genetic perturbation produces pleiotropic manifestations. Several features of the vascular phenotype are the reverse of SHORT syndrome, displaying vascular and soft tissue overgrowth as opposed to short stature, reduced adipose tissue, and tissue underdevelopment observed in SHORT syndrome. Divergent clinical phenotypes are determined by the nature of the *PIK3R1* alteration, the specificity of the consequences for PIK3Cα- and PIK3Cδ-mediated effects, and the timing and distribution of the alteration during embryogenesis. Disease-associated *PIK3R1* variants are enriched for indel events in both cancer and vascular anomalies with overgrowth. Detection of such variants is bioinformatically challenging, and further complicated by non-standardized annotation of the variant nomenclature. As such, these indel events are subject to ascertainment bias with additional study needed to discern frequency. Furthermore, studies to elucidate the molecular mechanisms underlying pathogenic variation of *PIK3R1* with widely disparate clinical phenotypes, including both under- and overgrowth syndromes and immunoregulation, will unify our understanding of this critical cellular proliferation pathway and provide further insight into treatment.

DATA AVAILABILITY

Variant data has been deposited into the ClinVar database.

ACKNOWLEDGEMENTS

The authors thank the participating individuals and their families described in this manuscript for their support and cooperation and the NIH Intramural Sequencing Center for performing NGS capture and sequencing. LGB was supported by the intramural research program of the National Human Genome Research Institute, grants HG200328 and HG200388. RKS was supported by the Wellcome Trust, grant 210752/Z/18/Z.

AUTHOR INFORMATION

Conceptualization: CEC, BAD; Data Curation: NRB, MA, DJC; Formal Analysis: CEC, MZ, RKS, LGB, BAD; Methodology: CEC, JH, VM, LGB, BAD; Investigation: CEC, JH, MC, ME, JND, JJJ, MJL, CCC, IF, MT, AZ, HC, LLT; Resources: DJC, JH, MC, ME, JJJ, MJL, OMTD, CCC, IF, MT, AZ, HC, LLT; Validation: CEC, VM, JJJ, MJL, LGB; Visualization: CEC, KVC; Writing-original draft: CEC, MA, VM, RKS, LGB, BAD; Writing- review and editing: CEC, RKS, LGB, BAD, OMTD; Supervision: CEC, LGB, BAD

ETHICS DECLARATION

The work presented herein was considered by the institutional review boards (IRB) designated to oversee and monitor biomedical human subjects research at the NIH, Washington University School of Medicine, and the University of Wisconsin. The limited, de-identified data associated with individuals contributed by Washington University School of Medicine was deemed as non-human subjects research by the IRB. Consent for participating individuals contributed by the NIH and through the multi-institutional network falling under the IRB of record through the University of Wisconsin, including publication and photography, was obtained.

REFERENCES

1. Lindhurst MJ, Sapp JC, Teer JK, et al. A mosaic activating mutation in AKT1 associated with the Proteus syndrome. *The New England journal of medicine.* 2011;365(7):611-619.
2. Cottrell CE, Al-Kateb H, Bredemeyer AJ, et al. Validation of a next-generation sequencing assay for clinical molecular oncology. *The Journal of molecular diagnostics : JMD.* 2014;16(1):89-105.
3. Siegel DH, Cottrell CE, Streicher JL, et al. Analyzing the Genetic Spectrum of Vascular Anomalies with Overgrowth via Cancer Genomics. *The Journal of investigative dermatology.* 2018;138(4):957-967.
4. Mirzaa GM, Riviere JB, Dobyns WB. Megalencephaly syndromes and activating mutations in the PI3K-AKT pathway: MPPH and MCAP. *American journal of medical genetics Part C, Seminars in medical genetics.* 2013;163c(2):122-130.
5. Keppler-Noreuil KM, Sapp JC, Lindhurst MJ, et al. Clinical delineation and natural history of the PIK3CA-related overgrowth spectrum. *American journal of medical genetics Part A.* 2014;164a(7):1713-1733.
6. Hopkins BD, Goncalves MD, Cantley LC. Insulin-PI3K signalling: an evolutionarily insulated metabolic driver of cancer. *Nat Rev Endocrinol.* 2020;16(5):276-283.
7. Madsen RR, Vanhaesebroeck B, Semple RK. Cancer-Associated PIK3CA Mutations in Overgrowth Disorders. *Trends in molecular medicine.* 2018;24(10):856-870.
8. Vadas O, Burke JE, Zhang X, Berndt A, Williams RL. Structural basis for activation and inhibition of class I phosphoinositide 3-kinases. *Science signaling.* 2011;4(195):re2.
9. Cheung LW, Hennessy BT, Li J, et al. High frequency of PIK3R1 and PIK3R2 mutations in endometrial cancer elucidates a novel mechanism for regulation of PTEN protein stability. *Cancer discovery.* 2011;1(2):170-185.
10. Tate JG, Bamford S, Jubb HC, et al. COSMIC: the Catalogue Of Somatic Mutations In Cancer. *Nucleic acids research.* 2019;47(D1):D941-d947.
11. Chang MT, Asthana S, Gao SP, et al. Identifying recurrent mutations in cancer reveals widespread lineage diversity and mutational specificity. *Nat Biotechnol.* 2016;34(2):155-163.
12. Gao J, Chang MT, Johnsen HC, et al. 3D clusters of somatic mutations in cancer reveal numerous rare mutations as functional targets. *Genome Med.* 2017;9(1):4.
13. Richards S, Aziz N, Bale S, et al. Standards and guidelines for the interpretation of sequence variants: a joint consensus recommendation of the American College of Medical Genetics and Genomics and the Association for Molecular Pathology. *Genetics in Medicine.* 2015;17(5):405-423.
14. Engelman JA, Luo J, Cantley LC. The evolution of phosphatidylinositol 3-kinases as regulators of growth and metabolism. *Nature reviews Genetics.* 2006;7(8):606-619.
15. Fruman DA, Bismuth G. Fine tuning the immune response with PI3K. *Immunological reviews.* 2009;228(1):253-272.
16. Rivière JB, Mirzaa GM, O'Roak BJ, et al. De novo germline and postzygotic mutations in AKT3, PIK3R2 and PIK3CA cause a spectrum of related megalencephaly syndromes. *Nature genetics.* 2012;44(8):934-940.
17. Kurek KC, Luks VL, Ayturk UM, et al. Somatic mosaic activating mutations in PIK3CA cause CLOVES syndrome. *American journal of human genetics.* 2012;90(6):1108-1115.
18. Wentink M, Dalm V, Lankester AC, et al. Genetic defects in PI3Kδ affect B-cell differentiation and maturation leading to hypogammaglobulineamia and recurrent infections. *Clin Immunol.* 2017;176:77-86.
19. Sun M, Hillmann P, Hofmann BT, Hart JR, Vogt PK. Cancer-derived mutations in the regulatory subunit p85alpha of phosphoinositide 3-kinase function through the catalytic

subunit p110alpha. *Proceedings of the National Academy of Sciences of the United States of America.* 2010;107(35):15547-15552.
20. Oliver MD, Fernández-Acero T, Luna S, et al. Insights into the pathological mechanisms of p85α mutations using a yeast-based phosphatidylinositol 3-kinase model. *Biosci Rep.* 2017;37(2).
21. Fruman DA, Rommel C. PI3K and cancer: lessons, challenges and opportunities. *Nature reviews Drug discovery.* 2014;13(2):140-156.
22. Coulter TI, Chandra A, Bacon CM, et al. Clinical spectrum and features of activated phosphoinositide 3-kinase δ syndrome: A large patient cohort study. *J Allergy Clin Immunol.* 2017;139(2):597-606.e594.
23. Lucas CL, Chandra A, Nejentsev S, Condliffe AM, Okkenhaug K. PI3Kδ and primary immunodeficiencies. *Nature reviews Immunology.* 2016;16(11):702-714.
24. Dornan GL, Siempelkamp BD, Jenkins ML, Vadas O, Lucas CL, Burke JE. Conformational disruption of PI3Kδ regulation by immunodeficiency mutations in PIK3CD and PIK3R1. *Proceedings of the National Academy of Sciences of the United States of America.* 2017;114(8):1982-1987.
25. Jaiswal BS, Janakiraman V, Kljavin NM, et al. Somatic mutations in p85alpha promote tumorigenesis through class IA PI3K activation. *Cancer cell.* 2009;16(6):463-474.
26. Dyment DA, Smith AC, Alcantara D, et al. Mutations in PIK3R1 cause SHORT syndrome. *American journal of human genetics.* 2013;93(1):158-166.
27. Avila M, Dyment DA, Sagen JV, et al. Clinical reappraisal of SHORT syndrome with PIK3R1 mutations: toward recommendation for molecular testing and management. *Clinical genetics.* 2016;89(4):501-506.
28. Bravo García-Morato M, García-Miñaúr S, Molina Garicano J, et al. Mutations in PIK3R1 can lead to APDS2, SHORT syndrome or a combination of the two. *Clin Immunol.* 2017;179:77-80.
29. Cerami E, Gao J, Dogrusoz U, et al. The cBio cancer genomics portal: an open platform for exploring multidimensional cancer genomics data. *Cancer discovery.* 2012;2(5):401-404.
30. Gao J, Aksoy BA, Dogrusoz U, et al. Integrative analysis of complex cancer genomics and clinical profiles using the cBioPortal. *Science signaling.* 2013;6(269):pl1.
31. Ye K, Wang J, Jayasinghe R, et al. Systematic discovery of complex insertions and deletions in human cancers. *Nat Med.* 2016;22(1):97-104.
32. Ross RL, Burns JE, Taylor CF, Mellor P, Anderson DH, Knowles MA. Identification of mutations in distinct regions of p85 alpha in urothelial cancer. *PLoS One.* 2013;8(12):e84411.
33. Venot Q, Blanc T, Rabia SH, et al. Targeted therapy in patients with PIK3CA-related overgrowth syndrome. *Nature.* 2018;558(7711):540-546.

FIGURE LEGENDS

Figure 1.. Domain structure of the longest PIK3R1 protein product showing distribution of monogenic disease-associated variants. Variants described in this study in association with a vascular malformation/overgrowth phenotype (top row). Variants described as pathogenic or likely pathogenic in the ClinVar database (accessed 11-13-2020 and filtered to encompass only variation less than 51 bp and with a described genetic condition) associated with SHORT syndrome (middle row) or Activated PI3K-Delta Syndrome 2 (bottom row).

Figure 2. Patient photographs of characteristic clinical phenotype. A. Capillary venous malformation with limb overgrowth (Klippel-Trenaunay), B. Macrodactyly with sandal toe deformity

Figure 1

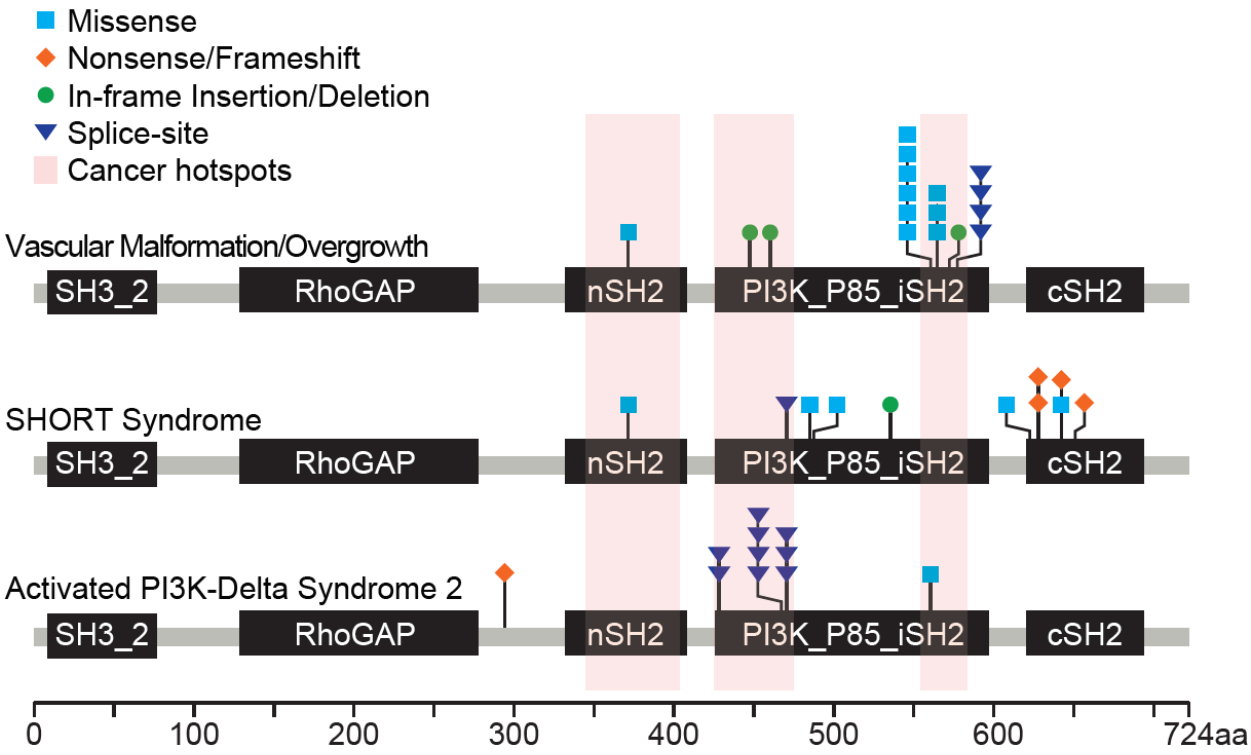

PIK3R1 NP_852664.1

Figure 2

Table I

***PIK3R1* Coding Variant (NM_181523.3)**	**Predicted Protein Consequence**	**Protein Domain**	**Tissue Type**	**Tissue Source**	**VAF; Total Depth at Variant Position**	**IND**
c.1126G>A	p.(Gly376Arg)	SH2	FT	PB; Reticulated port wine stain of left leg	2.9; 2772	13
c.1355_1365delinsTTCAAGAAAAAAGTTTCTTGAAA	p.(Tyr452_Gln455delinsPheGlnGluLysSerPheLeuLys)	PI3K_P85_iSH2	FFPE	EB; VM with features of AVM involving the epidermis/regional fibroadipose tissue on dorsum of left foot	6.4; 1086	17
c.1392_1403delTAGATTATATGA	p.(Asp464_Tyr467del)	PI3K_P85_iSH2	FT	Affected Skin	1.5; 1290	14
c.1690A>G	p.(Asn564Asp)	PI3K_P85_iSH2	CT	Affected Tissue	39.8*; 1224	1
c.1690A>G	p.(Asn564Asp)	PI3K_P85_iSH2	FT	Affected Tissue	24; 321	2
c.1690A>G	p.(Asn564Asp)	PI3K_P85_iSH2	FFPE	EB; Soft tissue mass consistent with a benign vascular malformation of the left forearm	3.4; 1980	3
c.1690A>G	p.(Asn564Asp)	PI3K_P85_iSH2	FT	PB; Affected Skin	2.8; 2779	10
c.1690A>G	p.(Asn564Asp)	PI3K_P85_iSH2	FT	PB; Affected Skin	2.2; 4159	12
c.1690A>G	p.(Asn564Asp)	PI3K_P85_iSH2	FT	PB; Affected Skin	1.8; 6616	16

c.1699A>G	p.(Lys567Glu)	PI3K_P85_iSH2	FT	PB; Affected Skin	4.1; 2675	4
c.1699A>G	p.(Lys567Glu)	PI3K_P85_iSH2	FT	PB; Affected Skin	2.3; 2737	9
c.1699A>G	p.(Lys567Glu)	PI3K_P85_iSH2	FT	PB; Affected Skin	1.1; 1425	11
c.1735_1740del CAATAC	p.(Gln579_Tyr580 del)	PI3K_P85_iSH2	FT	PB; Affected Skin	13.3; 1832	5
c.1746-6_1751del TTTCAGGTGGTT	p.(Met582_Asp60 5delinsIle)	PI3K_P85_iSH2	FT	PB; Affected Skin	3.1; 4205	6
c.1746-5_1748del TTCAGGTG	p.(Met582_Asp60 5delinsIle)	PI3K_P85_iSH2	FFPE	EB; Affected Skin	5.9; 1174	7
c.1748_1750delGGT	p.(Met582_Asp60 5delinsIle)	PI3K_P85_iSH2	FT	PB; Affected Skin	1.4; 2886	8
c.1748_1750delGGT	p.(Met582_Asp60 5delinsIle)	PI3K_P85_iSH2	FT	PB; Port wine stain of right forearm	2.2; 3317	15

FT= Fresh frozen tissue; FFPE= Formalin-fixed paraffin-embedded tissue; CT=cultured tissue; PB= Punch biopsy; EB= Excisional biopsy; VM= vascular malformation; AVM= arteriovenous malformation

* For individual 1, five samples of affected tissue were assayed by next-generation sequencing (NGS) or restriction fragment length polymorphism (RFLP) studies. Tissues including skin (NGS, 39.8% VAF; RFLP, 55.6% VAF), bone (RFLP, 26.49% VAF), cartilage (RFLP, 28.1% VAF), fat (RFLP, 0.96% VAF) and a mixed sample (RFLP, 1.25% VAF) were all cultured and DNA isolated from cultured cells was analyzed. Uncultured biopsy samples were not genotyped. Blood & unaffected fibroblasts were not observed to harbor the variant.

Table II

		Phenotypic Features								
IND	**Age (y)***	**DD**	**CM**	**LM**	**VM**	**OVG**	**Skeletal Abnormalities**	**Other Data**	***PIK3R1* Coding Variant (NM_181523.3)**	**Variant Classification and Type**
1	10	N	Y	Y	Y	Y	Macrodactyly, sandal gap	Fatty OVG	c.1690A>G	Pathogenic; Missense
2	5	N	Y	Y	Y	Y	Macrodactyly, Leg length discrepancy, sandal gap	Right congenital buphthalmos (congenital toxoplasmosis), Right anterior segment dysgenesis with glaucoma, Right microphthalmia	c.1690A>G	Pathogenic; Missense
3	6	NP	NP	NP	NP	NP	NP	Indication: Congenital malformation syndrome involving early overgrowth; Concern for CLOVES	c.1690A>G	Pathogenic; Missense
4**	17	N	Y	Y	Y	Y	Leg length discrepancy		c.1699A>G	Pathogenic; Missense
5	50	N	Y	Y	Y	Y	Macrodactyly, syndactyly	Lipoma	c.1735_1740delCAATAC	Pathogenic; In-frame Deletion
6	12	Y	Y	N	N	Y	N		c.1746-6_1751delTTTCAGGTGGTT	Pathogenic; Splice-site
7	30	N	Y	N	Y	Y	Macrodactyly, sandal gap		c.1746-5_1748delTTCAGGTG	Pathogenic; Splice-site
8	59	N	N	N	Y	Y	N		c.1748_1750delGGT	Pathogenic; Splice-site

9	21	N	Y	N	Y	Y	N		c.1699A>G	Pathogenic; Missense
10	18	N	Y	Y	Y	Y	N	Lipoma	c.1690A>G	Pathogenic; Missense
11	51	N	Y	N	Y	Y	Leg length discrepancy		c.1699A>G	Pathogenic; Missense
12	10	N	Y	Y	Y	Y	N	Frontal Bossing	c.1690A>G	Pathogenic; Missense
13	1	NP	NP	NP	NP	NP	NP	Indication: Reticulated port wine stain of left leg also affecting left side of scrotum; Left leg hypoplastic; Left testicular nubbin	c.1126G>A	Pathogenic; Missense
14	2	NP	NP	NP	NP	NP	NP	Indication: Klippel-Trenaunay syndrome	c.1392_1403del TAGATTATATGA	Likely Pathogenic; In-frame Deletion
15	20	NP	NP	NP	NP	NP	NP	Indication: Vascular nevus, hemihypertrophy	c.1748_1750delGGT	Pathogenic; Splice-site
16	39	N	Y	Y	Y	Y	N		c.1690A>G	Pathogenic; Missense
17	15	NP	NP	NP	NP	NP	NP	Indication: Klippel-Trenaunay syndrome; Vascular malformation and lipoma of left foot	c.1355_1365 delins TTCAAGAAAAAA GTTTCTTGAAA	Likely Pathogenic; In-frame Deletion

* Individual's age at time of enrollment in years

** Individual described previously in Siegel et al., 2018 (PMID: 29174369)

IND= Individual, DD= Developmental Delay, CM= Capillary Malformation, LM= Lymphatic Malformation, VM= Venous Malformation, OVG= Overgrowth, N= No; Y= Yes; NP= Not phenotyped by expert review, therefore indication for study listed in Other Data

Supplementary Material

Methodology

Primary and Washington University School of Medicine Cohorts

Sequencing studies of the primary cohort (consisting of a 16-institution collaborative network), and the Washington University School of Medicine cohort encompassed the methodologies described herein. Sequencing libraries were created following acoustic-focused fragmentation (Covaris), DNA end-repair, A-tailing, and indexing using the KAPA HyperPrep Kit (Roche Sequencing and Life Science KAPA Biosystems, Wilmington, MA) or Agilent SureSelect Library Kit (Agilent, Santa Clara, CA). Adapter-ligated DNA was subjected to limited-cycle amplification prior to target enrichment with either custom DNA or RNA capture probes (Integrated DNA Technologies, Coralville, IA or Agilent, respectively). Target capture space encompassed between 390 kb and 682 kb depending on assay version, ranging between 131-177 genes enriched for loci involved in cell signaling, oncogenesis and tumor suppression.

High-depth massively parallel sequencing was performed on Illumina instrumentation (Ilumina, Inc., San Diego, CA) to obtain short paired-end reads (101 or 151 bp) with average, unique on-target read depths of >1,000X across the capture space for high sensitivity in variant calling.

To orthogonally verify somatic variants at low allele frequency observed in *PIK3R1* in the primary cohort, two samples with available residual nucleic acid (representing disease-involved tissue from individual 4 and individual 6) were utilized for high-depth amplicon sequencing. *PIK3R1* primers were designed to encompass both the previously detected single nucleotide variant (SNV) in individual 4 and small deletion in individual 6 within a 296 bp PCR product: Forward primer 5'AGAAGCAGGCAGCTGAGTAT (GRCh37 chr5:67,591,056-67,591,075) and reverse primer 5'ATCTTCTGCTATCACCATCTTT (GRCh37 chr5:67,591,330-67,591,351). These amplified products were size confirmed, ligated with dual-match Illumina adapters (AGAAGGAC and AGAAGCCT, respectively) and re-amplified with Illumina universal P5/P7 primers. The amplicons were diluted to 50fM and sequenced on the Illumina MiniSeq.

Following massively parallel sequencing of captured libraries, BAM files were visualized using the Integrative Genomics Viewer[1] and demonstrated the expected SNV (c.1699A>G) and deletion event (c.1746-6_1751delTTTCAGGTGGTT) harbored by individuals 4 and 6, respectively. The c.1699A>G substitution (individual 4) was supported by 85 reads out of 2,259 total reads (3.8%). Amplicon sequencing data on individual 6 demonstrated reduced read support of 1526 averaged reads observed across positions chr5:67591239-67591250 representing the left-aligned deletion event in the BAM file. Immediately flanking this depressed read count value at chr5:67591238 and chr5:67591251, coverage increased to 1,655 reads supporting the small 12 bp deletion present at frequency of 7.8%.

The National Institutes of Health Cohort

The individuals evaluated at the NIH were first screened with a restriction fragment length polymorphism (RFLP) panel that tests for four common variants in *PIK3CA* and the c.49G>A p.(E17K) *AKT1* variant. RFLP negative samples were then reflexed to a custom capture next-generation sequencing (NGS) panel that interrogated >250 genes, including *PIK3R1,* and sequenced on an Illumina MiSeq instrument. The c.1690A>G variant in *PIK3R1* detected in individuals 1 and 2 was confirmed using a custom RFLP assay.

Variant Interpretation

Applicable criteria for the scoring of mosaic variation described within this cohort was adapted from Richards et al. as determined by CEC and LGB.[2]

Strong Evidence of Pathogenicity Criteria:

PS2

The observation of apparent somatic mosaicism was considered in the interpretation schema as applied to the existing de novo criteria in the American College of Medical Genetics and Genomics and the Association for Molecular Pathology (ACMG/AMP) standards and guidelines for variant interpretation.[2] Variants were considered to be of somatic etiology if a variant allele frequency/fraction (VAF) ranging between 1-25% was detected in a given sample or if a variant was present at differing frequencies among studied tissues from the same individual. Variants detected with a VAF of ≥ 3% as determined at the level of the coding variant (among any tested sample within the cohort in the case of recurrent coding variation), with no discernable strand bias, in regions absent of repetition, and sequence homology[3] and with clean, high-quality reads were considered as de novo events meeting strong criteria (PS2). Those variants at <3% VAF were considered as a moderate level of support of *de novo* status (PS2_Mod).

PS_Cancer

A novel strong criterion (PS_CANCER) was applied if the variant was well-represented in cancer as identified in the COSMIC database with ≥20 documented instances (cancer.sanger.ac.uk)[4] and considered to occur in a statistically significant hotspot or region (cancerhotspots.org)[5,6] within *PIK3R1*. This criterion was considered a moderate level of evidence if only one of the qualifiers (COSMIC or cancer hotspot) was met.

PS3

Functional studies were applied on the basis of available data in the literature using well-established models demonstrating downstream impact of the variant on RNA structure, gene expression or protein function.

Moderate Evidence of Pathogenicity Criteria:

PS4_Mod

At the level of the predicted amino acid change, the prevalence of the variant within our combined cohort was considered as a moderate level of evidence as applied in the setting of PS4 (prevalence of the variant in affected individuals is significantly increased compared with the prevalence in controls in the absence of a defined relative risk or odds ratio), with the observation of ≥5 unique occurrences in our cohort. PS4 was further downgraded to a supporting level of evidence where <5 and ≥3 unrelated individuals harbored the same predicted amino acid change within our cohort.

PM4

A moderate level of evidence criterion (PM4) was applied for protein length changes related to insertion/deletion events in a non-repeat region predicted to result in an in-frame protein product.

Supporting Evidence of Pathogenicity Criteria:

PP2

The criterion PP2 was applied for all *PIK3R1* missense variants due to constraint against missense changes in the gene, in the setting of a low rate of benign missense variation, given that missense changes are a common mechanism of both cancer and constitutional disease.

Criteria Not Applied:

PM2

Given the nature of the somatic variation under study, PM2 (absent from control or population databases) was not formally applied as evidence used in the setting of variant classification.

PP3

In silico prediction scores (PP3) were not applied due to the discordance in algorithms adequately identifying activating alterations.

References

1. Robinson JT, Thorvaldsdóttir H, Winckler W, et al. Integrative genomics viewer. *Nat Biotechnol.* Jan 2011;29(1):24-26.
2. Richards S, Aziz N, Bale S, et al. Standards and guidelines for the interpretation of sequence variants: a joint consensus recommendation of the American College of Medical Genetics and Genomics and the Association for Molecular Pathology. *Genetics in Medicine.* 2015/05/01 2015;17(5):405-423.
3. Mandelker D, Schmidt RJ, Ankala A, et al. Navigating highly homologous genes in a molecular diagnostic setting: a resource for clinical next-generation sequencing. *Genet Med.* Dec 2016;18(12):1282-1289.
4. Tate JG, Bamford S, Jubb HC, et al. COSMIC: the Catalogue Of Somatic Mutations In Cancer. *Nucleic acids research.* Jan 8 2019;47(D1):D941-d947.
5. Chang MT, Asthana S, Gao SP, et al. Identifying recurrent mutations in cancer reveals widespread lineage diversity and mutational specificity. *Nat Biotechnol.* Feb 2016;34(2):155-163.
6. Gao J, Chang MT, Johnsen HC, et al. 3D clusters of somatic mutations in cancer reveal numerous rare mutations as functional targets. *Genome Med.* Jan 23 2017;9(1):4.
7. Cerami E, Gao J, Dogrusoz U, et al. The cBio cancer genomics portal: an open platform for exploring multidimensional cancer genomics data. *Cancer discovery.* May 2012;2(5):401-404.
8. Gao J, Aksoy BA, Dogrusoz U, et al. Integrative analysis of complex cancer genomics and clinical profiles using the cBioPortal. *Science signaling.* Apr 2 2013;6(269):pl1.

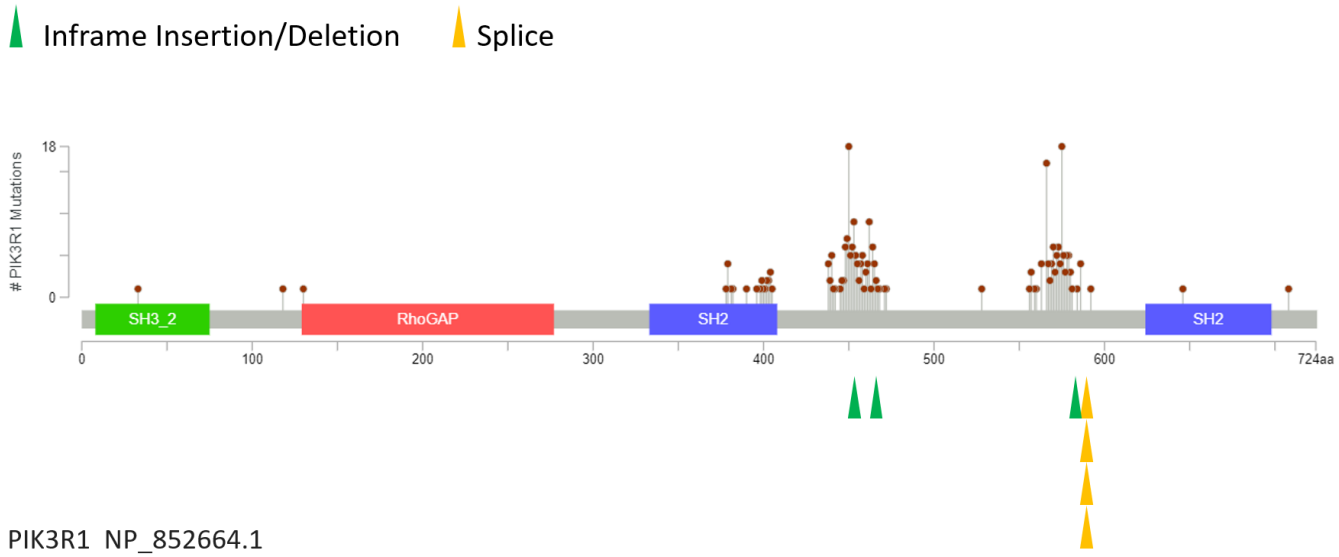

Supplementary Figure 1: Schematic Representation of *PIK3R1* Variants in Cancer and Vascular Malformation/Overgrowth

Plot demonstrating the frequency and location of insertion/deletion (indel) events in *PIK3R1* among a curated set of 181 non-redundant studies consisting of 47,580 cancer samples visualizable within cBioPortal (accessed 11-11-2020).[7,8] Indel hotspot events are clustered within the SH2 and inter-SH2 domains. Triangles highlight the frequency and location of indels among our multi-site cohort with vascular anomalies and overgrowth.

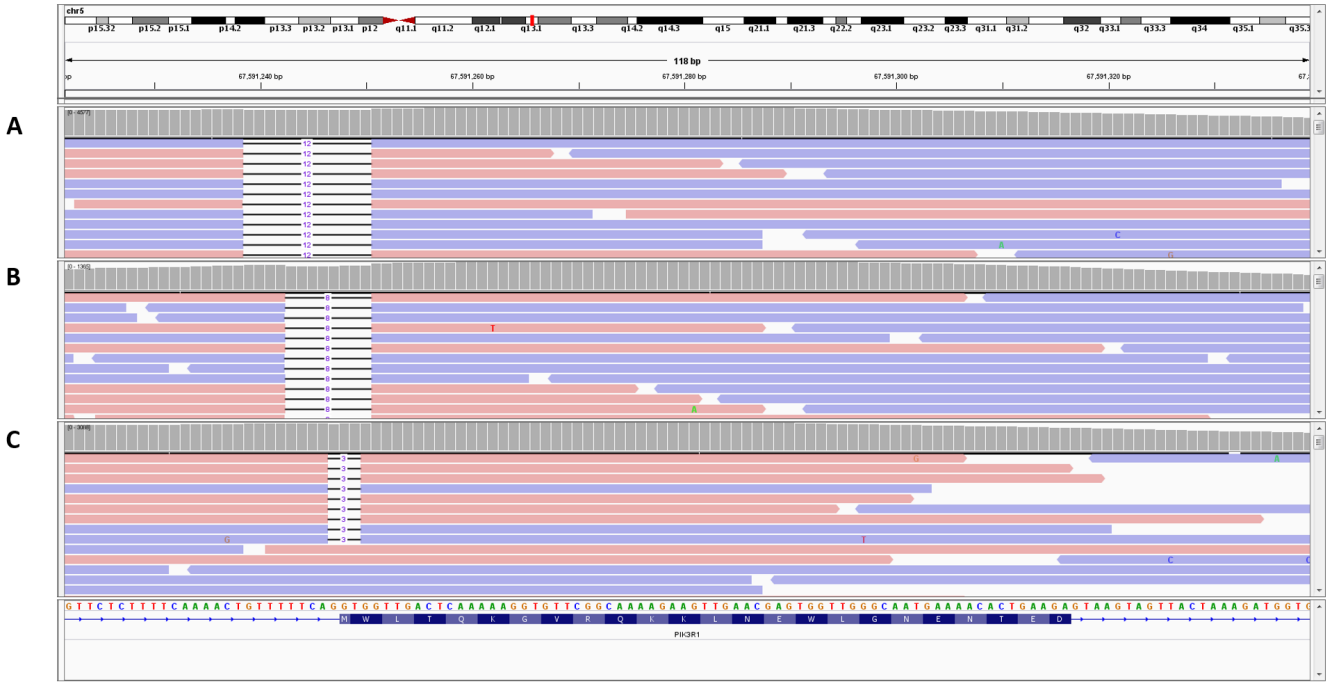

PIK3R1 NM_181523.3 Exon 14

Supplementary Figure 2: Splice-site Variants among Individuals with Vascular Malformation/Overgrowth as Visualized in Aligned Sequence Reads

Visualization within the Integrative Genomics Viewer (IGV)[1] of aligned reads in the BAM file derived from high-depth next-generation sequencing following target capture of the affected tissue of three individuals. A. Individual 6 harboring a 12 bp splice-site variant, B. Individual 7 harboring an 8 bp splice-site variant, C. Individual 8 harboring a 3 bp splice-site variant. These splice acceptor variants are predicted to encode an in-frame exon 14 skipping event, a described consequence of variants of this type in cancer.

Individual	*PIK3R1* DNA Variant GRCh37/hg19*	Location in Gene	*PIK3R1* Coding Variant (NM_181523.3)*
13	chr5:67589138G>A	Exon 10	c.1126G>A
17	chr5:67589592_67589602delinsTTCAAGAAAAAAGTTTCTTGAAA	Exon 11	c.1355_1365delinsTTCAAGAAAAAAGTTTCTTGAAA
14	chr5:67589629_67589640delTAGATTATATGA	Exon 11	c.1392_1403delTAGATTATATGA
1	chr5:67591097A>G	Exon 13	c.1690A>G
2	chr5:67591097A>G	Exon 13	c.1690A>G
3	chr5:67591097A>G	Exon 13	c.1690A>G
10	chr5:67591097A>G	Exon 13	c.1690A>G
12	chr5:67591097A>G	Exon 13	c.1690A>G
16	chr5:67591097A>G	Exon 13	c.1690A>G
4	chr5:67591106A>G	Exon 13	c.1699A>G
9	chr5:67591106A>G	Exon 13	c.1699A>G

11	chr5:67591106A>G	Exon 13	c.1699A>G
5	chr5:67591142_67591142delCAATAC	Exon 13	c.1735_1740delCAATAC
6	chr5:67591242_67591253delTTTCAGGTGGTT	Intron13/ Exon 14 Junction	c.1746-6_1751delTTTCAGGTGGTT
7	chr5:67591243_67591250delTTCAGGTG	Intron13/ Exon 14 Junction	c.1746-5_1748delTTCAGGTG
8	chr5:67591250_67591252delGGT	Intron13/ Exon 14 Junction	c.1748_1750delGGT
15	chr5:67591250_67591252delGGT	Intron13/ Exon 14 Junction	c.1748_1750delGGT

*As per Human Genome Variation Society (HGVS) nomenclature conventions, for all variant descript

**PI3K_P85_iSH2 = Phosphatidylinositol 3-kinase regulatory subunit P85 inter-SH2 domain

*** FT= Fresh Frozen Tissue; FFPE= Formalin-Fixed Paraffin-Embedded Tissue; CT= Cultured Tissue

^^ For deletion variants, base position 5' of deletion start used for depth count

[a]COSMIC (v88) https://cancer.sanger.ac.uk/cosmic (Accessed 4-7-2019) (PMID: 30371878)

[b]cancerhotspots.org (accessed 11-8-2020) (PMID: 26619011; 28115009)

[c]varsome.com (PMID: 30376034) All variant attributes were manually curated through the use of ge

[d]*PIK3R1* deletions occuring within the PI3K_p85_iSH2 domain among a region of frequent insertior

[e]Deletion events matched on genomic coordinates in COSMIC

Predicted Protein Consequence*	Variant Classification (ACMG/AMP Modified Criteria)	ClinVar Accession
p.(Gly376Arg)	Pathogenic (PS_CANCER, PS3, PS2_Mod, PP2)	SCV001478395
p.(Tyr452_Gln455delinsPheGlnGluLysSerPheLeuLys)	Likely Pathogenic (PS2, PM_CANCER, PM4)	SCV001478396
p.(Asp464_Tyr467del)	Likely Pathogenic (PS2_Mod, PM_CANCER, PM4)	SCV001478397
p.(Asn564Asp)	Pathogenic (PS_CANCER, PS2, PS3, PS4_Mod, PP2)	SCV001478398
p.(Asn564Asp)	Pathogenic (PS_CANCER, PS2, PS3, PS4_Mod, PP2)	SCV001478398
p.(Asn564Asp)	Pathogenic (PS_CANCER, PS2, PS3, PS4_Mod, PP2)	SCV001478398
p.(Asn564Asp)	Pathogenic (PS_CANCER, PS2, PS3, PS4_Mod, PP2)	SCV001478398
p.(Asn564Asp)	Pathogenic (PS_CANCER, PS2, PS3, PS4_Mod, PP2)	SCV001478398
p.(Asn564Asp)	Pathogenic (PS_CANCER, PS2, PS3, PS4_Mod, PP2)	SCV001478398
p.(Lys567Glu)	Pathogenic (PS_CANCER, PS2, PS4_Sup, PP2)	SCV001478399
p.(Lys567Glu)	Pathogenic (PS_CANCER, PS2, PS4_Sup, PP2)	SCV001478399

p.(Lys567Glu)	Pathogenic (PS_CANCER, PS2, PS4_Sup, PP2)	SCV001478399
p.(Gln579_Tyr580del)	Pathogenic (PS2, PS3, PM_CANCER, PM4,)	SCV001478400
p.(Met582_Asp605delinsIle)	Pathogenic (PS2, PS3, PM_CANCER, PM4, PS4_Sup)	SCV001478401
p.(Met582_Asp605delinsIle)	Pathogenic (PS2, PS3, PM_CANCER, PM4, PS4_Sup)	SCV001478402
p.(Met582_Asp605delinsIle)	Pathogenic (PS2, PS3, PM_CANCER, PM4, PS4_Sup)	SCV001478403
p.(Met582_Asp605delinsIle)	Pathogenic (PS2, PS3, PM_CANCER, PM4, PS4_Sup)	SCV001478403

ions the most 3’ position possible of the reference sequence is arbitrarily assigned to have been changed

enomic databases and literature, with Varsome.com used as one such interface to access links to data sou

n/deletion events

Variant Type	Protein Domain**	Tissue Sequenced***	Variant Allele Frequency/ Fraction (VAF)% by NGS	Assay Methodology
Missense	SH2	FT	2.9	NGS Gene Panel Custom Capture
Inframe Deletion	PI3K_P85_iSH2	FFPE	6.4	NGS Gene Panel Custom Capture
Inframe Deletion	PI3K_P85_iSH2	FT	1.5	NGS Gene Panel Custom Capture
Missense	PI3K_P85_iSH2	CT	39.8	NGS Gene Panel Custom Capture; RFLP Variant Verification
Missense	PI3K_P85_iSH2	FT	24	NGS Gene Panel Custom Capture; RFLP Variant Verification
Missense	PI3K_P85_iSH2	FFPE	3.4	NGS Gene Panel Custom Capture
Missense	PI3K_P85_iSH2	FT	2.8	NGS Gene Panel Custom Capture
Missense	PI3K_P85_iSH2	FT	2.2	NGS Gene Panel Custom Capture
Missense	PI3K_P85_iSH2	FT	1.8	NGS Gene Panel Custom Capture
Missense	PI3K_P85_iSH2	FT	4.1	NGS Gene Panel Custom Capture; NGS High Depth Amplicon Variant Verification
Missense	PI3K_P85_iSH2	FT	2.3	NGS Gene Panel Custom Capture

Missense	PI3K_P85_iSH2	FT	1.1	NGS Gene Panel Custom Capture
Inframe Deletion	PI3K_P85_iSH2	FT	13.3	NGS Gene Panel Custom Capture
Splice-site	PI3K_P85_iSH2	FT	3.1	NGS Gene Panel Custom Capture; NGS High Depth Amplicon Variant Verification
Splice-site	PI3K_P85_iSH2	FFPE	5.9	NGS Gene Panel Custom Capture
Splice-site	PI3K_P85_iSH2	FT	1.4	NGS Gene Panel Custom Capture
Splice-site	PI3K_P85_iSH2	FT	2.2	NGS Gene Panel Custom Capture

(3'rule) (PMID: 26931183)

rces and to serve as a visualization of local sequence context

Read Depth at Variant Position^^	Reference/Alternate allele depth (read strand counts)	Documented in COSMIC - Identical amino acid change/Any missense change at codon (%)[a]	Cancer Hotspot (Y/N); (Q-value) cancerhotspots.org[b]
2772	2689 (1483+; 1206-) / 81 (44+;37-)	26/27 (96.3%) COSM35827	Y- (1.68×10^{-19})
1086	1002 (527+; 475-) / 83 (48+; 35-)	0 (0%)[d]	Y- (9.35×10^{-183})
1290	1274 (658+; 616-)/ 15 (2+; 13-)	14/14 (100%)[e] COSM3736943, COSM4714460, COSM4714461, COSM87228	Y- (9.35×10^{-183})
1224	734 (392+; 342-) / 490 (267+; 223-)	41/43 (95.3%) COSM42912	Y- (1.08×10^{-23})
321	243 (119+; 124-) / 78 (39+; 39-)	41/43 (95.3%) COSM42912	Y- (1.08×10^{-23})
1980	1911 (958+; 953-) / 68 (31+; 37-)	41/43 (95.3%) COSM42912	Y- (1.08×10^{-23})
2779	2697 (1363+; 1334-)/ 78(40+; 38-)	41/43 (95.3%) COSM42912	Y- (1.08×10^{-23})
4159	4062 (2058+;2004-)/ 93 (55+;38-)	41/43 (95.3%) COSM42912	Y- (1.08×10^{-23})
6616	6494 (3252+; 3242-)/ 118 (56+;62-)	41/43 (95.3%) COSM42912	Y- (1.08×10^{-23})
2675	2563 (1286+; 1277-)/ 111 (55+; 56-)	33/33 (100%) COSM1069611	Y-(3.35×10^{-17})
2737	2674 (1341+; 1333-)/ 62 (29+;33-)	33/33 (100%) COSM1069611	Y-(3.35×10^{-17})

1425	1408 (713+;695-)/ 15(11+;4-)	33/33 (100%) COSM1069611	Y-(3.35×10^{-17})
1832	1572 (695+;876-)/ 245(101+;144-)	0 (0%)[c]	Y- (8.13×10^{-89})
4205	4083 (2023+, 2060-)/ 131 (60+, 71-)	0 (0%)[c]	Y- (3.86×10^{-13})
1174	1096 (622+; 474-)/ 68(43+;25-)	0 (0%)[c]	Y- (3.86×10^{-13})
2886	2845 (1362+; 1483-)/ 40 (21+; 19-)	3/3 (100%)** COSM2157179	Y- (3.86×10^{-13})
3317	3225 (1716+; 1509-) / 90 (45+; 45-)	3/3 (100%)** COSM2157179	Y- (3.86×10^{-13})

VarSome Variant Search Engine Link[c]
https://varsome.com/variant/hg19/NM_181523.3(PIK3R1)%3Ac.1126G%3EA
https://varsome.com/variant/hg19/chr5%2067589591%20.%20TATAACACTCAG%20TTTCAAGAAAAAAGTTTCTTGAAA
https://varsome.com/variant/hg19/5%3A67589623%3A12%3A
https://varsome.com/variant/hg19/NM_181523.3(PIK3R1)%3Ac.1690A%3EG
https://varsome.com/variant/hg19/NM_181523.3(PIK3R1)%3Ac.1690A%3EG
https://varsome.com/variant/hg19/NM_181523.3(PIK3R1)%3Ac.1690A%3EG
https://varsome.com/variant/hg19/NM_181523.3(PIK3R1)%3Ac.1690A%3EG
https://varsome.com/variant/hg19/NM_181523.3(PIK3R1)%3Ac.1690A%3EG
https://varsome.com/variant/hg19/NM_181523.3(PIK3R1)%3Ac.1690A%3EG
https://varsome.com/variant/hg19/NM_181523.3(PIK3R1)%3Ac.1699A%3EG
https://varsome.com/variant/hg19/NM_181523.3(PIK3R1)%3Ac.1699A%3EG

https://varsome.com/variant/hg19/NM_181523.3(PIK3R1)%3Ac.1699A%3EG
https://varsome.com/variant/hg19/5%3A67591140%3A6%3A
https://varsome.com/variant/hg19/5%3A67591239%3A12%3A
https://varsome.com/variant/hg19/5%3A67591243%3A8%3A
https://varsome.com/variant/hg19/5%3A67591247%3A3%3A
https://varsome.com/variant/hg19/5%3A67591247%3A3%3A